ELASTIC TORQUES ABOUT MEMBRANE EDGES

A Study of Pierced Egg Lecithin Vesicles

SILKE LORENZEN, ROLF-M. SERVUSS, AND WOLFGANG HELFRICH
Fachbereich Physik, Freie Universität Berlin, Arnimallee 14, D-1000 Berlin 33, Federal Republic of Germany

ABSTRACT The shape of mechanically pierced giant vesicles is studied to obtain the elastic modulus of Gaussian curvature of egg lecithin bilayers. It is argued that such experiments are governed by an apparent modulus, $\bar{\kappa}_{app}$, not the true modulus of Gaussian curvature, $\bar{\kappa}$. A theory of $\bar{\kappa}_{app}$ is proposed, regarding the pierced bilayer vesicle as a closed monolayer vesicle. The quantity measured, i.e. $\bar{\kappa}_{app}/\kappa$, where κ is the rigidity, agrees satisfactorily with the theory. We find $\bar{\kappa}_{app} = -(1.9 \pm 0.3) \cdot 10^{-12}$ erg (on the basis of $\kappa = (2.3 \pm 0.3) \cdot 10^{-12}$ erg). The result may have implications for bilayer fusion.

INTRODUCTION

The curvature elastic energy of fluid layers, in its usual quadratic approximation, is governed by two elastic moduli. One of them, the bending rigidity κ, has been obtained (1–5) for the bilayers of some lecithins, in particular those of egg lecithin, by analyzing the shape fluctuations of vesicles. The other modulus, $\bar{\kappa}$, is associated with Gaussian curvature. The integral of this curvature over a closed surface depends only on the genus (6), i.e., the number of handles, of the surface (Gauss-Bonnet theorem). It changes in steps of -4π with the topology, e.g., in going from a sphere to a torus. As a result, Gaussian curvature cannot cause any surface torques and forces in the membrane, but it will give rise to line torques and forces acting along imaginary or real cuts through the membrane.

It is tempting to assume the bending elastic energy and the line torques of bilayers to be determined by membrane shape and the elastic moduli κ and $\bar{\kappa}$. The energies of circular disks and spherical caps have, in fact, been expressed by Helfrich (7) and Fromherz (8) in terms of κ, $\bar{\kappa}$, and an edge energy or line tension γ. Derzhanski et al. (9) did a first estimate of $\bar{\kappa}$ for egg lecithin. It is based on a theoretical instability of disks with respect to sphering, the minimum size of sonicated vesicles, and experimental values for γ and κ (see below). Mitov (private communication) tried to obtain $\bar{\kappa}$ from the membrane curvatures at the rim of the hole of electrically opened egg lecithin vesicles (10), assuming a vanishing elastic line torque about the membrane edge.

When we started to pierce giant vesicles with a needle to derive $\bar{\kappa}$, like Mitov, from the membrane curvatures next to the hole, we realized that current concepts are most probably naive, supposing the edge to behave like a clean cut with the hydrocarbon chains in contact to water. The energy of such an edge seems prohibitive in view of the large hydrocarbon/water interface. If the edge has a different structure, e.g., connects the two monolayers, we may have to replace the true bilayer modulus, $\bar{\kappa}$, by an apparent modulus of Gaussian curvature, $\bar{\kappa}_{app}$, when dealing with bilayer edges. The equations for membrane energy and boundary torques need not change their forms, although the elastic energy associated with $\bar{\kappa}_{app}$ may reside in the curved edge rather than the curved membrane.

This paper is a study of $\bar{\kappa}_{app}$, both experimental and theoretical. We begin with a theory of the bending elastic energies of membranes and their edges. The approach taken here is to regard the pierced bilayer vesicle, including the membrane edge, as a closed monolayer vesicle. In the framework of the model we show that indeed the equations do not change while $\bar{\kappa}$ is replaced by a well-defined $\bar{\kappa}_{app}$. With a view to the experiments, the boundary torque balance relating $\bar{\kappa}_{app}/\kappa$ to the ratio of the principal curvatures at the membrane edge is formulated such as to allow for an interaction with the needle. Subsequently, we describe the experiments in which egg lecithin membranes were pierced with micromanipulated glass and tungsten needles under a phase contrast microscope. The measured value of $\bar{\kappa}_{app}$ agrees rather well with the theoretical prediction. There is also satisfactory agreement with the estimate employing the minimum size of sonicated vesicles. Finally, we discuss a slight dependence of $\bar{\kappa}_{app}$ on needle radius and in this context the interaction between needle and membrane edge. The significance of our results for the fusion of egg lecithin bilayers is considered in the conclusion.

THEORY

The curvature elastic energy per unit area, g, of a fluid surface that may be a bilayer or a monolayer is usually

written as (11)

$$g = \frac{1}{2} \kappa (c_1 + c_2 - c_0)^2 + \bar{\kappa} c_1 c_2, \qquad (1)$$

where c_1 and c_2 are the principal curvatures, c_0 the spontaneous curvature, and κ and $\bar{\kappa}$ the elastic moduli. The product $c_1 c_2$ is called Gaussian curvature and corresponds to saddle splay in liquid crystals. In conformity with Eq. 1, our calculations will be restricted to a quadratic approximation in the curvatures unless otherwise stated.

The monolayers of a bilayer are assumed to slide freely on each other. In the following, bilayer moduli are unmarked, monolayer moduli are distinguished by the superscript m (κ^m, $\bar{\kappa}^m$), while c_0 exclusively denotes monolayer spontaneous curvature. (The spontaneous curvature of the pierced bilayer is thought to vanish.) Spontaneous curvature c_0 and the modulus $\bar{\kappa}^m$ can be nonzero if the stress profile of the flat monolayer contains regions of counterbalancing push and pull (12, 13). The net lateral tensions as well as monolayer stretching will be regarded as negligible.

A bilayer vesicle with one hole is topologically equivalent to a closed monolayer vesicle if the two monolayers composing the bilayer are connected at the edge of the membrane. An edge structure of this type is sketched in Fig. 1. The total integral of Gaussian curvature over the monolayer vesicle is 4π. It can be split into two parts, one taken over the strongly curved edge region and the other over the weakly bent monolayers of the bilayer membrane, as illustrated by Fig. 2. We may write

$$\int_{\text{edge}} c_1 c_2 \, dA + 2 \int_{\text{mem}} c_1 c_2 \, dA = 4\pi \qquad (2)$$

where in the edge region the integral is over the neutral
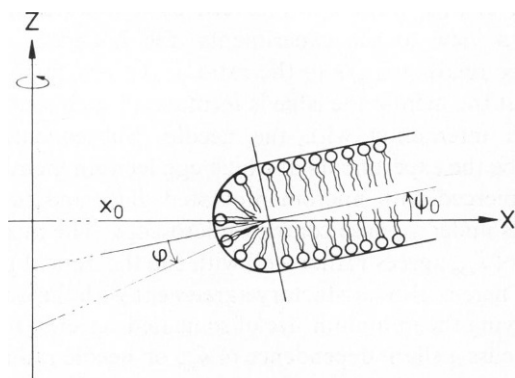
FIGURE 1 Proposed structure of bilayer edge surrounding a circular hole. The neutral surface, not shown, should lie within the monolayer. ψ_0 is the edge angle, i.e., the angle between the membrane tangent at the hole and the normal to the rotation axis. For practical purposes it makes no difference whether x_0 is the radius of the needle, or of the core line (see text), or of another line in the edge (as here). The function $c(\phi)$ introduced in the text depends on the position of the line.
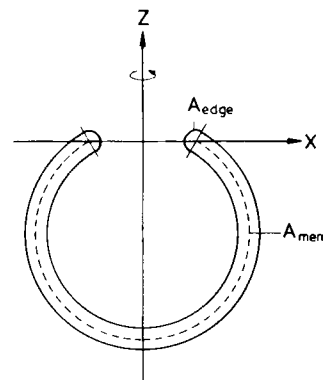
FIGURE 2 Schematic drawing of rotationally symmetric pierced bilayer vesicle represented by closed monolayer vesicle. The solid lines indicate the neutral surfaces of the inner and outer monolayers. The membrane area, A_{mem}, indicated by the dashed line, lies in the middle between the neutral surfaces. A_{edge} is the area of the neutral surface in the edge region.

surface of the monolayer, i.e. the surface where the mean molecular cross section equals that in the flat state. Outside the edge region the integral over the monolayers is expressed by twice the integral over the membrane, or the central surface between the monolayer neutral surfaces, and its curvatures. Eq. 2 will permit us to replace certain integrals over the edge by integrals over the membrane and vice versa.

We are interested in the total curvature elastic energy of the pierced vesicle $G = G_{\text{mem}} + G_{\text{edge}}$. The energy of the membrane without edge (or with an edge like a cut) may be cast in the form

$$G_{\text{mem}} = 2 \left[\frac{1}{2} \kappa^m \int_{\text{mem}} (c_1 + c_2)^2 \, dA + \frac{1}{2} \kappa^m \int_{\text{mem}} c_0^2 \, dA \right.$$
$$\left. + \bar{\kappa}^m \int_{\text{mem}} c_1 c_2 \, dA \right] - 2\kappa^m a c_0 \int_{\text{mem}} c_1 c_2 \, dA, \quad (3)$$

employing monolayer material parameters. The curvature of the outer monolayer of a spherical membrane is defined as positive. The length a is the (constant) spacing of the monolayers, more precisely of their neutral surfaces. The last term of Eq. 3 takes into account that the contributions of the two monolayers to the integral of $c_0(c_1 + c_2)$ do not cancel completely. Although cubic in curvatures, it cannot be dropped, as c_0 can be much larger than c_1 and c_2. An easy way of checking the last term, in particular its Gaussian character, is to calculate the energy in question directly for a sphere and a cylinder. It is nonzero for the sphere but zero for the cylinder. The bilayer modulus of Gaussian curvature is, according to Eq. 3

$$\bar{\kappa} = 2\bar{\kappa}^m - 2\kappa^m a c_0. \qquad (4)$$

An extensive derivation of this relationship has been given by Petrov and Bivas (12). Finally, we suppose $|ac_0| \ll$ so that a quartic correction of the second term of Eq. 3, also of

Gaussian character, can be neglected. (It would drop out anyway below.)

Let us assume now that the curvature in an orthogonal cross section of the edge depends on the angle ϕ as indicated in Fig. 1 ($c(-\phi) = c(\phi)$), but is independent of whether the edge is a straight or curved line. This ensures that $c(\phi)$ is always a principal curvature, say c_1, which of course is very strong. It is then advantageous to decompose the elastic energy of the edge as follows

$$G_{edge} = \frac{1}{2} \kappa^m \int_{edge} (c_1^2 - 2c_1 c_o)\, dA + \frac{1}{2}\kappa^m \int_{edge} c_o^2\, dA$$
$$+ \frac{1}{2}\kappa^m \int_{edge} c_2^2\, dA + \kappa^m \int_{edge} c_2(c_1 - c_o)\, dA$$
$$+ \bar{\kappa}^m \int_{edge} c_1 c_2\, dA. \qquad (5)$$

We assign to the edge a fixed width and define a core line $\mathbf{r}(s)$, which lies in its central surface at a fixed distance from its vertex. The variable s measures the length of the line. The distance is chosen such that the contribution of the first term of Eq. 5 per ds remains unchanged if the line is curved. (The line curvature is reflected in c_2; it could affect the considered term through dA whenever its curvature vector $d^2\mathbf{r}/ds^2$ has a component in the tangent plane of the membrane.) The first term of Eq. 5 may now be identified with γL, where γ is the edge energy per unit length, also called line tension, and L the total length of the line. The third term of Eq. 5 represents a bending energy of the edge that does not generally vanish, but should be negligible as compared to other terms of G in experiments with large circular holes. Omitting it, we are left with

$$G_{edge} = \gamma L + \frac{1}{2}\kappa^m \int_{edge} c_o^2\, dA + \kappa^m \int_{edge} c_2(c_1 - c_o)\, dA$$
$$+ \bar{\kappa}^m \int_{edge} c_1 c_2\, dA. \qquad (6)$$

Adding Eqs. 3 and 6 results in

$$G = \gamma L + \kappa^m \int_{mem} (c_1 + c_2)^2\, dA + \kappa^m \int_{edge} c_1 c_2\, dA$$
$$- 2\kappa^m a c_o \int_{mem} c_1 c_2\, dA - \kappa^m c_o \int_{edge} c_2\, dA. \qquad (7)$$

Note that the two $\bar{\kappa}^m$ terms no longer appear since because of Eq. 2 their sum is a constant, and can thus be dropped. Assuming the monolayer to be unstretchable, we have also lost the two c_o^2 terms that together form another constant.

The simplest conceivable model of the membrane edge is a semi-cylindrical monolayer joining the two membrane monolayers. Closure of the edge then requires $c_1 = 2/a$ all over the edge. In this model the distance between core line and vertex is $(a/2)(1 - 2/\pi)$ and the natural choice for the width of the edge is $a/2$. (Not only the edge energy but also the edge area is conserved when this edge is bent.) Using

Eq. 2 again, we combine the last term and half the fourth of Eq. 7 into an integral over the edge,

$$\kappa^m c_o \int_{edge} \left(\frac{a}{2}c_1 - 1\right) c_2\, dA, \qquad (8)$$

plus a further constant. The integral vanishes if $c_1 = 2/a$ is inserted. The semicylinder model may not be quite realistic as the monolayer is likely to bulge at the membrane edge for reasons of molecular packing (14). However, it is assumed here to be valid for the sake of simplicity. Deviations from it would affect in the following Eq. 10 only the term proportional to c_o. The other, more important term is independent of the details of edge structure.

Collecting the remaining nonconstant terms of Eq. 7 and using the obvious equality $\kappa = 2\kappa^m$, we arrive at

$$G = \gamma L + \frac{1}{2}\kappa \int_{mem} (c_1 + c_2)^2\, dA + \bar{\kappa}_{app} \int_{mem} c_1 c_2\, dA, \qquad (9)$$

where

$$\bar{\kappa}_{app} = -\kappa\left(1 + \frac{a}{2}c_o\right). \qquad (10)$$

The energy of the last term of Eq. 9 resides in the edge rather than the membrane. Nevertheless, we prefer the representation in terms of membrane integrals since the same equation, with $\bar{\kappa}$ instead of $\bar{\kappa}_{app}$, holds for a cutlike edge possessing no curvature elastic energy of its own. In such a model, γL would be the energy of the hydrocarbon/water interface along the membrane edge. The real membrane edge may differ from both the naive model of a cut and the monolayer-vesicle model, especially its quadratic approximation. We expect Eq. 9 to hold in any case, with $\bar{\kappa}_{app}$ depending on edge structure.

A formula permitting us to obtain $\bar{\kappa}_{app}$ from experiment is derived next. For this purpose we consider a rotationally
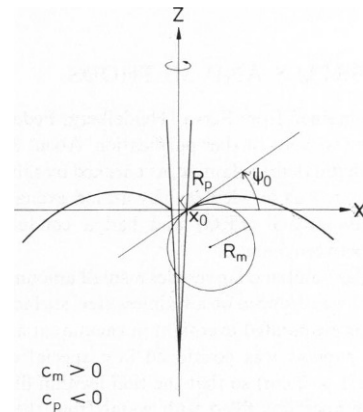
FIGURE 3 Cross section of a vesicle with inserted needle assuming rotational symmetry. x_o is the radius of the hole (or the needle at the position of the hole), ψ_0 is the edge angle. It is positive for clockwise rotation. R_m and R_p are the radii of principal curvatures (the largest and the smallest), $c_m = 1/R_m$ and $c_p = 1/R_p$.

symmetric piece of membrane with a hole of radius x_0 at one pole as shown in Fig. 3. With ψ_0 being the edge angle, i.e., the angle between the tangent to the membrane contour at the hole and the normal to the rotation axis, the two principal curvatures are the meridional curvature $c_m = \cos \psi_0 d\psi/dx$, and the parallel curvature $c_p = \sin \psi_0/x_0$. The internal torque per unit length acting about the membrane edge is given by the derivative of Eq. 1 with respect to meridional curvature,

$$\tau_i = \frac{\partial g_c}{\partial c_m} = \kappa(c_m + c_p) + \bar{\kappa}_{app} c_p, \quad (11)$$

where, as in Eq. 9, $\bar{\kappa}_{app}$ takes the place of $\bar{\kappa}$. The spontaneous curvature should vanish because of equal media inside and outside the membrane and the possibility of the monolayer molecular densities equilibrating via the edge. (These are, of course, preconditions for the monolayer-vesicle model to be applicable.)

The torques per unit length of membrane edge can be the sum of an external line torque τ_e and an internal line torque τ_i. The total torque vanishes, i.e.,

$$\tau_e + \tau_i = 0, \quad (12)$$

if the membrane is in mechanical equilibrium. In the absence of external torques acting on the membrane one has $\tau_i = 0$. Because of Eq. 11 the ratio of the elastic moduli is then

$$\frac{\bar{\kappa}_{app}}{\kappa} = -\left(1 + \frac{c_m}{c_p}\right). \quad (13)$$

Accordingly, $\bar{\kappa}_{app}$ can be derived if κ is known and c_m and c_p are measured. If an external torque exists, the ratio is given by

$$\frac{\bar{\kappa}_{app}}{\kappa} = -\left(1 + \frac{c_m}{c_p}\right) - \frac{\tau_e}{\kappa c_p}. \quad (14)$$

MATERIALS AND METHODS

Egg lecithin was obtained from Serva (Heidelberg, Federal Republic of Germany) and used without further purification. About 30% of the head groups were phosphatidylethanolamine, as checked by thin layer chromatography (15). Water was ion-depleted by an ion exchanger (Seradest, Scral, Ransbach-Baumbach, FRG) and had a conductivity of <0.1 μS/cm and a pH between 5 and 6.

For preparing giant unilamellar vesicles a small amount of egg lecithin dissolved in ethanol was dropped on a stainless steel surface (2 × 10 mm), and the ethanol was evaporated overnight in vacuum at a temperature of ~70°C. Then the support was positioned in a special chamber (inner height 2 mm, base 1 × 2 cm) so that the thin lecithin film was oriented vertically. The chamber was filled with water from the open side and mounted on the stage of the microscope. The lecithin swelled at room temperature and formed unilamellar and multilamellar vesicles. After >1 h a suitable vesicle (unilamellar, diameter between 100 and ~200 μm) was selected and opened by a thin needle made of glass or tungsten.

The glass needles were pulled from 1-mm glass tubes in a micropipette puller (E. Leitz, Wetzlar, FRG) to outer tip diameters of ~1 μm or more. The tungsten needles were prepared by electrolysis in an electrolyte bath

of satured potassium nitrite solution with currents of 1–2 A DC until minimal radii of 1 μm were reached. The microneedles could be mounted on a pipette holder of a micromanipulator (E. Leitz) and moved in the chamber by a mechanically acting control lever. The geometric parameters of the needles, their diameters and conicities, were determined from the video image. The optical resolution was 0.4 μm in the object plane. The angles β between needle axis and the conical surface lay between 0° and 13.5° (see Table I) and were determined with an uncertainty of ±0.5°.

All observations were made at room temperature with a phase-contrast microscope (E. Leitz) and simultaneously recorded on video tape (Grundig). The lamellarity of the vesicles, i.e., the number of bilayers in the vesicle wall, was determined from the contrast of the video image of the vesicle's contour. For that purpose the intensity distribution along video lines perpendicular to the contour of the vesicle wall was analyzed by means of a line selector (Grundig, Fürth, FRG) and a digital storage oscilloscope (Tektronix, Inc., Beaverton, OR). The optical contrast of vesicle walls has been shown to depend on lamellarity and radius (16, 17). Our apparatus was calibrated by measuring the contrast of >30 giant vesicles. In the resulting diagram of contrast vs. radius, the group with smallest contrast could be clearly distinguished from the rest and was associated with unilamellarity. Photographs of opened vesicles were analyzed with the help of a semi-automatic image analyzer (MOP-Videoplan, Kontron, Oberkochen, FRG). The contour coordinates were obtained with a digitizer tableau, and the principal curvatures of the membrane near the hole were computed by numerical fitting. The ratio of the elastic moduli given below represents the average of the two sides if the rotational symmetry was imperfect.

OBSERVATIONS AND RESULTS

During the swelling of egg lecithin a great variety of vesicular structures developed from the thin lecithin film. We saw vesicles that moved freely in the aqueous phase, while other membranes stayed in contact with the steel surface. Sometimes we observed giant, almost planar membranes with curvatures <50 cm^{-1}, which spanned the whole visible part of the chamber. Small vesicles mostly drifted away when approached by the needle, but larger

TABLE I
SELECTED DATA OF ELEVEN VESICLES

No.	x_0	R_v	ψ_0	β	c_m	$\bar{\kappa}_{app}/\kappa$
	μm		degrees	degrees		μm
1	1.3	75	−11	1.5	−0.025	−0.82 ± 0.06
2	1.5	80	−54	0	−0.022	−0.95 ± 0.03
3	1.6	100	13	<1	−0.016	−0.97 ± 0.1
4	1.9	≫100	38	9	−0.014	−0.96 ± 0.02
5	2.2	45	−43	2	−0.031	−0.90 ± 0.04
6	3.0	75	−19	5.5	−0.054	−0.70 ± 0.05
7	4.5	60	−35.5	13	−0.035	−0.73 ± 0.06
8	4.9	≫100	37	6	−0.021	−0.82 ± 0.05
9	5.0	85	−31.5	13.5	−0.039	−0.63 ± 0.07
10	5.3	≫100	47.5	10	−0.025	−0.82 ± 0.05
11	2.6	≫100	−24.5	2	−0.026	−0.84 ± 0.08

Only one needle position is considered for each vesicle. The vesicles were pierced with glass (1–10) and tungsten (11) needles. x_0 is the radius of the hole in the membrane, e.g. the needle radius at the position of the membrane hole. R_v is the radius of the vesicle. ψ_0 is the edge angle (see Fig. 1), with $\psi_0 < 0$ indicating an inward funnel. β is the conicity of the needle, i.e. the angle between axis and surface of the needle. c_m is the meridional curvature of the membrane at the position of the hole.

ones did not so readily escape. They could be pressed against the vertical steel support and were often deeply dented without being pierced. In some cases, however, the needle perforated the vesicle wall. The membrane edge often manifested itself by a very faint line across the needle. The contours of the membranes near the hole could point inwards or outwards as illustrated by Figs. 4 and 5. We remark that outward funnels were observed only with open (pipette-like) needles that gave both inward and outward funnels with the same vesicles. All the bilayers showed undulations with amplitudes up to a few micrometers before and after being pierced, which indicates that the lateral tensions were extremely small ($\leq 10^{-5}$ dyn/cm) (18). The membrane edges were not seen to fluctuate.

If the slightly conical needles were moved horizontally, the membrane edges came into contact with different needle diameters. The membranes relaxed within 20–50 s to a new (quasi) stationary position, where they remained until further needle movements. Thus it was possible to analyze membrane contours with different hole radii for a single vesicle. Although the membrane edges seemed to slide easily over the needle they may have settled in
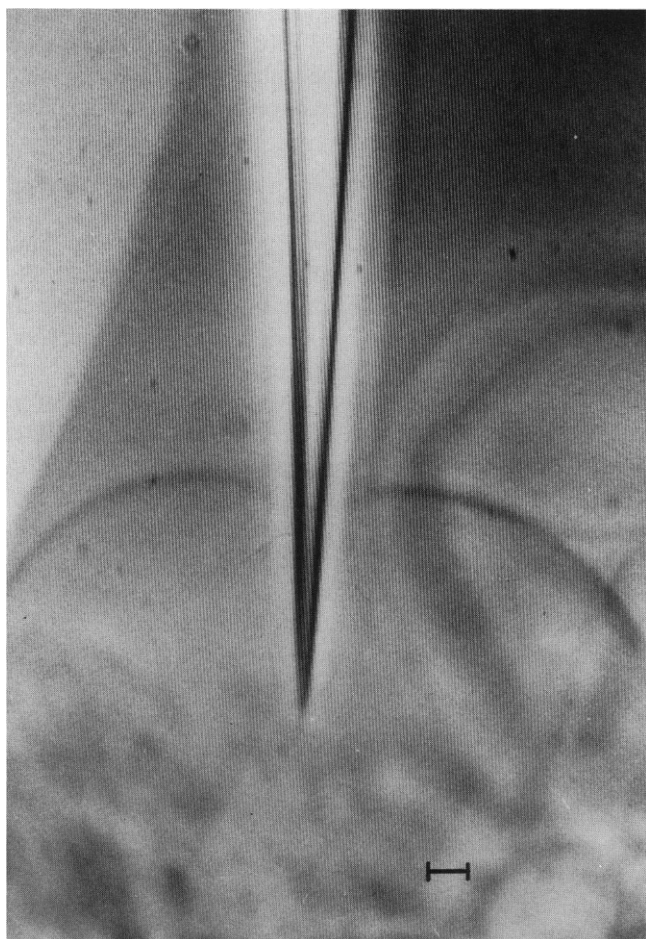
FIGURE 4   Photograph of a video image of a pierced vesicle forming inward funnel. The bar represents 10 μm.
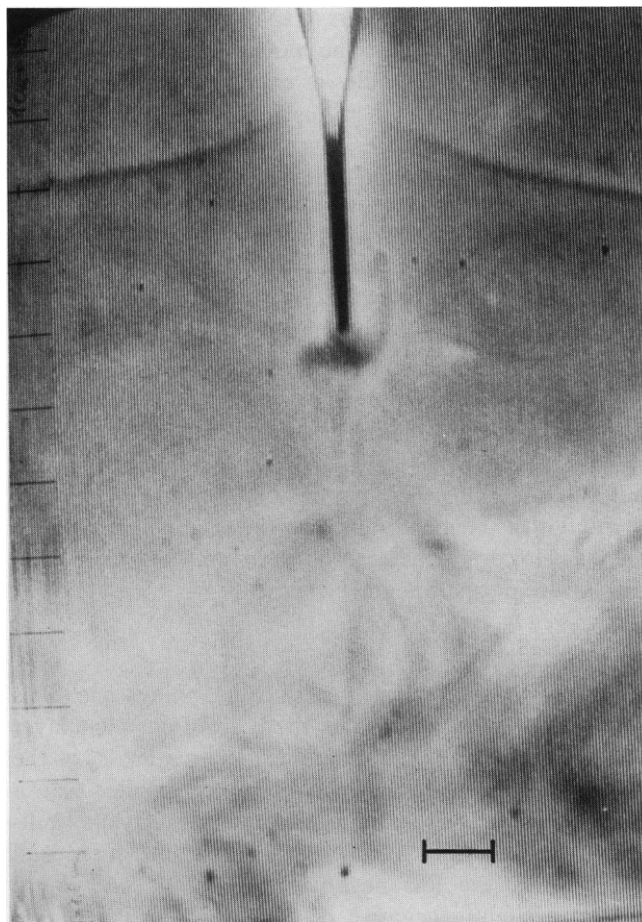
FIGURE 5   Photograph of a video image of a pierced vesicle forming outward funnel. The bar represents 10 μm.

nonequilibrium positions (see below). Electron micrographs of a glass needle revealed a pronounced surface roughness, with some protrusions reaching a height of 100 nm. When the needle was drawn out of a vesicle the membrane sometimes slid off the needle, in other cases a thin lecithin tether was pulled out of the membrane.

The apparent modulus of Gaussian curvature of pierced unilamellar vesicles was calculated with Eq. 13 from 17 experiments that were carried out with 11 different vesicles. The vesicle diameters ranged from 90 μm to >200 μm, and the needle diameters at the position of the hole ranged from 1.3 to 5.3 μm. We obtained ratios $\bar{\kappa}_{app}/\kappa$ between −0.63 and −0.97 with a mean value of −0.83 and a standard deviation of 0.12, which was about as large as the estimated error of the single experiments resulting from imperfect rotational symmetry and other uncertainties. With the curvature elastic modulus $\kappa = (2.3 \pm 0.3) \cdot 10^{-12}$ erg (1) the apparent modulus of Gaussian curvature for pierced unilamellar egg lecithin membranes in water at room temperature comes out to be $\bar{\kappa}_{app} = -(1.9 \pm 0.3) \cdot 10^{-12}$ erg.

The data of representative experiments, one with each of the 10 vesicles opened with glass needles, are summarized

in Table I. The last line refers to an experiment carried out with a tungsten needle. The values for $\bar{\kappa}_{app}/\kappa$ show no dependence on vesicle radius or edge angle, but there is a slight correlation with the radius x_0 of the membrane hole. If we assume a linear dependence of the ratio of moduli on the hole radius as suggested by Eq. 14 for fixed angle ψ_0, extrapolation to $x_0 = 0$ yields for the 10 representative experiments of Table I performed with glass needles $\bar{\kappa}_{app}(0)/\kappa = -0.98 \pm 0.07$. Figs. 6 and 7 show the results obtained with two single vesicles when the hole radius was varied, the needles being of glass and tungsten, respectively. Extrapolation to zero radius leads to $\bar{\kappa}_{app}(0)/\kappa -0.76 \pm 0.04$ with the tungsten needle. The slopes of the linear fits are positive in the case of glass (Table I and Fig. 6), while a negative slope is found in the case of tungsten (Fig. 7). The difference may result from a small specific interaction of the membrane with the needle material (see below). However, the dependences on hole radius lie almost within experimental error.

DISCUSSION

The measured ratio $\bar{\kappa}_{app}/\kappa$ nearly equals minus one. This may have been anticipated on the basis of our monolayer model, i.e., Eq. 10. The spontaneous curvature c_0 of the egg-lecithin monolayer is probably much smaller than a typical edge curvature, considering the bilayer's well-known stability. The fact that all $\bar{\kappa}_{app}/\kappa$, measured and extrapolated, are less negative than minus one might suggest a slightly negative c_0. However, the use of the quadratic theory of monolayer bending elasticity up to the extreme curvatures of the membrane edge is likely to impair the validity of Eq. 10. Elastic energy terms of higher than second order in the curvatures (19) may enter for which no data are available. Also, a bulging of the edge which was assumed to be semicylindrical may reduce the effect of spontaneous curvature on $\bar{\kappa}_{app}$ in comparison with Eq. 10. In any event, the apparent modulus $\bar{\kappa}_{app}$ can differ from the true bilayer modulus of Gaussian curvature of Eq. 4. Earlier attempts (9, 20, 21) to evaluate the modulus of Gaussian curvature did not differentiate between $\bar{\kappa}$ and $\bar{\kappa}_{app}$. (There remain ambiguities even if the distinction is made.) The estimate of the modulus of Gaussian curvature
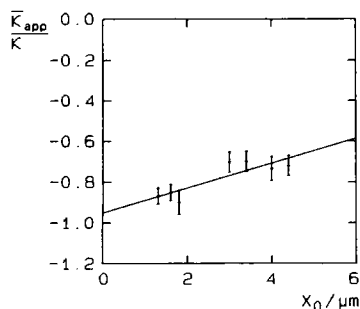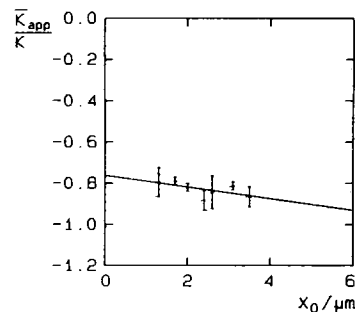
FIGURE 7   Plot of $\bar{\kappa}_{app}/\kappa$ as obtained from Eq. 13 vs. hole radius. All data from a single vesicle pierced with a tungsten needle.

by Derzhanski et al. (9) should actually give $\bar{\kappa}_{app}$ instead of $\bar{\kappa}$. We repeat it here with slightly different numbers. It is based on the formula

$$r_c = 2(2\kappa + \bar{\kappa}_{app})/\gamma \qquad (15)$$

for the maximum size of a circular disk that is stable with respect to sphering (7). Note that r_c is the radius of the sphere made from the disk, the radius of the latter would be twice as large. Inserting $\kappa = 2 \cdot 10^{-12}$ erg (1, 5), $\gamma = 2 \cdot 10^{-6}$ dyn (10), and $r_c = 100$ Å, the approximate minimum radius of sonicated vesicles (22) (all found with egg lecithin), one derives $\bar{\kappa}_{app} = -3 \cdot 10^{-12}$ erg. Alternatively, one may identify r_c with the sphere radius for which circular disk and closed sphere have the same energy. The resulting equation

$$r_c = (2\kappa + \bar{\kappa}_{app})/\gamma \qquad (16)$$

and the above numbers yield $\bar{\kappa}_{app} = -2 \cdot 10^{-12}$ erg. The agreement with our measured $\bar{\kappa}_{app}$ is better than can be expected from such a crude estimate. It becomes poorer if one takes the values of γ obtained by other authors (23, 24), which are about half the quoted one.

It should be mentioned that even the largest value of γ measured, $2 \cdot 10^{-6}$ dyn, is four times less than the line tension calculated for the semicylinder model (13) with $\kappa^m = 1 \cdot 10^{-12}$ erg, $c_0 = 0$, and $a = 4$ nm. Bulging of the edge may reduce the tension, but can hardly account for all of the discrepancy. At least in principle, the edge can have an energy lower than calculated from bending elasticity by reason of its thermal fluctuations.

An infinitely extended membrane pierced by a strictly cylindrical needle should assume a flat configuration whenever $\bar{\kappa}_{app} < 0$. This is its state of minimum elastic energy, regardless of which model applies: the naive model (no distinction between $\bar{\kappa}$ and $\bar{\kappa}_{app}$), the monolayer vesicle model ($\bar{\kappa}$ and $\bar{\kappa}_{app}$ linked only through c_0) or a mixed model, each with a different distribution of the elastic energy over membrane and edge. The inward or outward funnels that we usually saw around conical and cylindrical needles should, therefore, be nonequilibrium states. We believe that the membrane edges became easily hooked on the needle surfaces. They may have been held in place by the

FIGURE 6   Plot of $\bar{\kappa}_{app}/\kappa$ as obtained from Eq. 13 vs. hole radius. All data from a single vesicle pierced with a glass needle.

combination of a line tension with a surface roughness, which in the case of glass was verified (see above). Most of the needles used were conical enough to expect a slipping membrane to be stripped. This follows from a simple comparison of the energies of line contraction and vesicle deformation. The fact that the edges around conical needles also came to a halt, even in the case of outward funnels, is further evidence for a readiness of the edges to hook on the needle surface.

The shapes of pierced vesicles can be quasistationary as any elastic forces due to membrane curvature are very weak. At least in the case of very extended membranes they are unlikely to bring about significant changes of the enclosed volume during an experiment. Any lateral tensions appeared too low to disturb the measurement of the curvatures next to the walls.

The ratio of the principal curvatures at the membrane edge and thus $\bar{\kappa}_{app}/\kappa$ depended very little on the needle radius. This suggests that no significant external torques arose from the interaction of membrane edges and needle surfaces. The curvature elastic torques per unit length should be inversely proportional to the hole radius, given a fixed edge angle and zero lateral tension. The interaction with the wall may produce torques per unit length that depend differently or not at all on hole radius. Our linear extrapolation of $\bar{\kappa}_{app}/\kappa$ to zero radius conforms with the assumption that any external torques per unit length are independent of hole radius (see Eq. 14). Straightforward estimates indicate that thermal fluctuations can locally pull the membrane edge away from the needle, a typical separation being 2 nm for the radius $x_0 = 1$ μm. Fluctuations of this kind, while keeping the edges hooked, help to understand the virtual absence of an external boundary torque originating from an interaction with the needle surface. However, a variation of the total length of membrane edge with edge angle would also bring about an external torque. Apparently, any change in length was small enough to be insignificant (a membrane thickness or less).

CONCLUSION

In our experiments with egg lecithin bilayers we have found a negative apparent modulus of Gaussian curvature, $\bar{\kappa}_{app}$, of about the same magnitude as the bending rigidity. The large negative value means that around a hole an extended membrane prefers the flat configuration. Membrane pores, i.e., very small holes, may be expected to display the same tendency if the monolayers are still connected by them. Such hydrophilic pores are thus unlikely to form the funnels envisaged by Petrov and Mitov (25) as possible precursors of membrane fusion. Fusion remains energetically favored if the true modulus of Gaussian curvature, $\bar{\kappa}$, is positive (13, 21), but the process of fusion should take a different route. Recent experiments with egg lecithin and similar materials seem to indicate

that the first step of membrane fusion is monolayer fusion involving one monolayer of either bilayer (24, 26, 27).

The measured value of $\bar{\kappa}_{app}$ agrees well with a theory regarding the pierced bilayer vesicle as a closed monolayer vesicle and employing monolayer bending elasticity. The validity of our simple model remains to be tested by experiments with other materials. It is obvious, and there is evidence (10, 24, 28), that the edge energy can be lowered by admixtures that accumulate in the edge region. The monolayer-vesicle model may also hold in these cases (if the concentration of the additive is proportional to monolayer curvature $c_1 + c_2$). However, it is conceivable that there are agents that change the boundary more drastically, producing low-energy edges with $\bar{\kappa}_{app} \approx \bar{\kappa}$ so that funnels could be preferred over flat pores. The new method of analyzing the shape of pierced vesicles seems suitable to examine this.

REFERENCES

1. Servuss, R. M., W. Harbich, and W. Helfrich. 1976. Measurement of the curvature-elastic modulus of egg lecithin bilayers. Biochim. Biophys. Acta. 436:900–903.
2. Schneider, M. B., J. T. Jenkins, and W. W. Webb. 1984. Thermal fluctuations of large cylindrical phospholipid vesicles. Biophys. J. 45:891–899.
3. Schneider, M. B., J. T. Jenkins, and W. W. Webb. 1984. Thermal fluctuations of large quasi-spherical bimolecular phospholipid vesicles. J. Phys. (Paris). 45:1457–1472.
4. Engelhardt, H., H. P. Duwe, and E. Sackman. 1985. Bilayer bending elasticity measured by Fourier analysis of thermally excited surface undulations of flaccid vesicles. J. Phys. Lett. 46:L-395–L-400.
5. Beblik, G., R. M. Servuss, and W. Helfrich. 1985. Bilayer bending rigidity of some synthetic lecithins. J. Phys. (Paris). 46:1773–1778.
6. Stoker, J. J. 1969. Differential geometry. Wiley-Interscience, New York.
7. Helfrich, W. 1974. The size of bilayer vesicles generated by sonication. Phys. Lett. 50A:115–119.
8. Fromherz, P. 1983. Lipid-vesicle structure: size control by edge-active agents. Chem. Phys. Lett. 94:259–266.
9. Derzhanski, A., A. G. Petrov, and M. D. Mitov. 1978. Molecular asymmetry and saddle-splay elasticity in lipid bilayers. Ann. Phys. (Paris). 3:297–298.
10. Harbich, W., and W. Helfrich. 1979. Alignment and opening of giant lecithin vesicles by electric fields. Z. Naturforsch. 34a:1063–1065.
11. Helfrich, W. 1973. Elastic properties of lipid bilayers: theory and possible experiments. Z. Naturforsch. 28c:693–703.
12. Petrov, A. G., and I. Bivas. 1985. Elastic and flexoelectric aspects of out-of-plane fluctuations in biological and model membranes. Prog. Surf. Sci. 16:389–511.
13. Helfrich, W. 1981. Amphiphilic mesophases made of defects. In Physics of Defects. R. Balian, editor. Les Houches, Session XXXV. 1980. Elsevier, North Holland. 716–755.
14. Mitchell, D. J., and B. W. Ninham. 1981. Micelles, vesicles and microemulsions. J. Chem. Soc. Farad. Trans. II. 77:601–629.

15. Servuss, R. M. 1984. Lichtmikroskopische Untersuchungen zur Undulations-Wechselwirkung grosser Lecithin-Vesikeln. Doctoral Thesis, Freie Universität, Berlin.

16. Servuss, R. M., and E. Boroske. 1979. Lamellarity of artificial phospholipid-membranes determined by photometric phase-contrast microscopy. *Phys. Lett.* 69A:468–470.

17. Servuss, R. M., and E. Boroske. 1980. Dependence of the optical contrast of vesicle walls on lamellarity and curvature. *Chem. Phys. Lipids.* 27:57–69.

18. Helfrich, W., and R. M. Servuss. 1984. Undulations, steric interaction, and cohesion of fluid membranes. *Nuovo Cimento D.* 3:137–151.

19. Mitov, M. D. 1978. Third and fourth order curvature elasticity of lipid bilayers. *Comp. Rend. Acad. Bulg. Sci.* 31:513–515.

20. Petrov, A. G., M. D. Mitov, and A. Derzhanski. 1978. Saddle splay instability in lipid bilayers. *Phys. Lett.* 65A:374–376.

21. Harbich, W., R. M. Servuss, and W. Helfrich. 1978. Passages in lecithin-water systems. *Z. Naturforsch.* 33a:1013–1017.

22. Cornell, B. A., G. C. Fletcher, J. Middlehurst, and F. Separovic. 1982. The lower size limit to the size of small sonicated phospholipid vesicles. *Biochim. Biophys. Acta.* 690:15–19.

23. Taupin, C., M. Dvolaitzky, and C. Sauterey. 1975. Osmotic pressure induced pores in phospholipid vesicles. *Biochemistry.* 14:4771–4775.

24. Chernomordik, L. V., M. M. Kozlov, G. B. Melikyan, I. G. Abidor, V. S. Markin, and Yu. A. Chizmadzhev. 1985. The shape of lipid molecules and monolayer membrane fusion. *Biochim. Biophys. Acta.* 812:643–655.

25. Petrov, A. G., and M. D. Mitov. 1982. Defects in lipid bilayers and their influence on membrane fusion. *Stud. Biophys.* 90:223–225.

26. Horn, R. G. 1984. Direct measurement of the force between two lipid bilayers and observation of their fusion. *Biochim. Biophys. Acta.* 778:224–228.

27. Fisher, L. R., and N. S. Parker. 1984. Osmotic control of bilayer fusion. *Biophys. J.* 46:253–258.

28. Fromherz, P., and D. Rüppel. 1985. Lipid vesicle formation: the transition from open shell to closed disk. *FEBS (Fed. Eur. Biochem. Soc.) Lett.* 179:155–159.